Proline Isomerization in Bovine Pancreatic Ribonuclease A. 2. Folding Conditions†

Rajiv Bhat,‡ William J. Wedemeyer, and Harold A. Scheraga*

Baker Laboratory of Chemistry and Chemical Biology, Cornell University, Ithaca, New York 14853-1301

Received January 24, 2003; Revised Manuscript Received March 28, 2003

ABSTRACT: The kinetics of cis−trans isomerization of individual X−Pro peptide groups is used to study the backbone dynamics of bovine pancreatic ribonuclease A (RNase A). We previously developed and validated a fluorescence method for monitoring the cis−trans isomerization of the Tyr92−Pro93 and Asn113−Pro114 peptide groups of RNase A under *unfolding* conditions [Juminaga, D., Wedemeyer, W. J., and Scheraga, H. A. (1998) *Biochemistry 37*, 11614−11620]. The essence of this method is to introduce a fluorescent residue (Tyr or Trp) in a position adjacent to the isomerizing proline (if one is not already present) and to eliminate the fluorescence of other such residues adjacent to prolines by mutating them to phenylalanine. Here, we extend this method to observe the cis−trans isomerization of these peptide groups under *folding* conditions using two site-directed mutants (Y92F and Y115F) of RNase A. Both isomerizations decelerate with increasing concentrations of GdnHCl, with nearly identical *m* values (1.11 and 1.19 M^{-1}, respectively) and extrapolated zero-GdnHCl time constants (42 and 32 s, respectively); by contrast, under *unfolding* conditions, the cis−trans isomerizations of both Pro93 and Pro114 are independent of GdnHCl concentration. Remarkably, the isomerization rates under *folding* conditions at GdnHCl concentrations above 1 M are significantly slower than those measured under *unfolding* conditions. The temperature dependence of the Pro114 isomerization under folding conditions is also unusual; whereas Pro93 exhibits an activation energy typical of proline isomerization (19.4 kcal/mol), Pro114 exhibits a sharply reduced activation energy of 5.7 kcal/mol. A structurally plausible model accounts for these results and, in particular, shows that folding conditions strongly accelerate the cis−trans isomerization of both peptide groups to their native cis conformation, suggesting the presence of flickering local structure in their β-hairpins.

The cis−trans isomerization of peptide groups (especially X−Pro peptide groups) has several properties that make it attractive for a study of the effects of backbone perturbations on protein folding (*1*). First, it is a localized, structurally simple, two-state transition with a high activation energy (20 kcal/mol) and a well-defined reaction coordinate (the peptide dihedral angle ω). Under unfolding conditions, cis−trans isomerization of peptide groups is relatively insensitive to denaturant concentrations and pH (*2*, *3*), although it can be catalyzed by reducing the double-bond character of the C′−N bond, e.g., by reducing the polarity of the solvent (*4*), by protonating the prolyl nitrogen with strong acids (*5*), by donating a hydrogen bond to the prolyl nitrogen (*6*), or by introducing electron-withdrawing substituents on the proline ring (*7*). Second, cis−trans isomerization is generally much slower than conformational folding, making it possible to characterize the folding of individual isomeric species (*1*, *2*, *8*). Nonnative cis−trans isomers of different peptide groups within the same protein can have grossly different effects on the folding rate; for example, the incorrect isomer of the Tyr92−Pro93 peptide group of RNase[1] A can retard the folding rate 500-fold, whereas other incorrect isomers have no effect at all (*1*). For comparison, side-chain mutations rarely cause a more than 20-fold change in the folding rate (*9*−*11*).

Having characterized the effects of nonnative proline isomers on the conformational folding rate (*1*), we now study the converse problem, i.e., the effects of folding conditions on the rates of proline isomerization. The imposition of solution conditions that promote conformational folding is likely to change the rate of cis−trans isomerization by altering the backbone dynamics and, thus, the "attempt frequency" (i.e., the average rate at which a crossing of the transition state is attempted); this corresponds to a change in the activation entropy $\Delta S^{\ddagger}$. In principle, the activation enthalpy $\Delta H^{\ddagger}$ for cis−trans isomerization could also change with solution conditions, if they alter the double-bond character of the C′−N bond; however, since the denaturant concentration seems to have little effect on isomerization rates under unfolding conditions (*2*, *3*), we neglect this effect and attribute changes in the cis−trans isomerization rates to changes in the backbone dynamics. However, it is not clear whether the isomerization rate under folding conditions will be greater or smaller than that under unfolding conditions.

† This work was supported by NIH Grant GM-24893. R.B. was the recipient of a Department of Biotechnology, Government of India, overseas associateship during the tenure of this work at Cornell University.

* To whom correspondence should be addressed. Telephone: (607) 255-4034. Fax: (607) 254-4700. E-mail: has5@cornell.edu.

‡ Present address: Centre for Biotechnology, Jawaharlal Nehru University, New Delhi 110 067, India.

[1] Abbreviations: RNase, bovine pancreatic ribonuclease A; GdnHCl, guanidine hydrochloride.

10.1021/bi030024t CCC: $25.00
Published on Web 04/26/2003

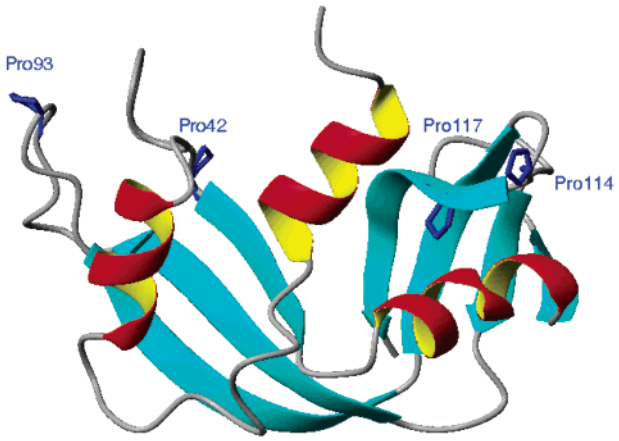

FIGURE 1: Ribbon diagram of bovine pancreatic ribonuclease A, with the four prolines (Pro42, Pro93, Pro114, and Pro117) indicated. This figure was prepared with MOLMOL (*15*).

Our model protein is bovine pancreatic ribonuclease A (RNase A), which has been studied extensively in our laboratory (*1*) and others (*12*, *13*). RNase A has four prolines, two cis in the native state (Pro93 and Pro114) and two trans (Pro42 and Pro117) (*14*) [Figure 1 (*15*)]. Exhaustive site-directed mutagenesis and folding studies have shown that Pro42, Pro114, Pro117, and Pro93 cause increasing disruption of conformational folding (*1*); whereas Pro42 and Pro114 have little effect, an incorrect Pro117 or Pro93 isomer retards folding by 50- or 500-fold, respectively (*1*, *2*, *8*).

We previously developed and validated a method for monitoring the individual cis−trans isomerizations of the Tyr92−Pro93 and Asn113−Pro114 peptide groups of RNase A by single-jump *unfolding* experiments (2). Specifically, we showed that the slow unfolding fluorescence phase of wild-type RNase A arises from two sources: Tyr92 reporting on the isomerization of the Tyr92−Pro93 peptide group and Tyr115 reporting on the isomerization of the Asn113−Pro114 peptide group. Exhaustive site-directed mutagenesis showed that other prolines and tyrosines do not contribute to the slow unfolding fluorescence phase, not even Pro117 which is two residues from Tyr115 (*2*). We further showed that the knockout mutations Y92F and Y115F do not affect the stability or folding of RNase A, but allow the two fluorescence signals (and, thus, the two proline isomerizations) to be monitored separately under *unfolding* conditions, with Y92F monitoring the isomerization around the Asn113−Pro114 peptide bond and Y115F monitoring the isomerization around the Tyr92−Pro93 peptide bond. The essence of our method is to introduce a fluorescent residue (Tyr or Trp) in a position adjacent to the proline of interest (if one is not already present) and to eliminate the fluorescence of other such residues next to prolines by mutating them to phenylalanine.

We apply this method here to observe the cis−trans isomerization of these peptide groups under *folding* conditions. This is accomplished by a double-jump procedure of the type U → F → U (U being unfolded and F the folded state of the protein), in which the protein is initially unfolded, subjected to folding conditions for a variable time *t*, and finally returned to unfolding conditions. In the final (F → U) step, conformational unfolding occurs much more rapidly than the isomerization, producing a biphasic fluorescence signal; the faster phase corresponds to unfolding without isomerization, whereas the slower phase corresponds to isomerization after unfolding is completed. If only one proline is adjacent to a fluorescent residue, the slower fluorescence phase corresponds to the isomerization of that proline (*2*); thus, the slow unfolding fluorescence phases of the Y92F and Y115F mutants of RNase A report on the isomerizations of Pro114 and Pro93, respectively. The amplitudes of these slow unfolding phases are proportional to the percentage of peptide groups that undergo isomerization during the final unfolding step (F → U). Hence, the amplitudes measured in double-jump experiments (U → F → U) correspond to the differences between the cis/trans percentages in the unfolded state and those that have developed after folding for a time *t* in the U → F step.

The Tyr92−Pro93 and Asn113−Pro114 peptide groups are particularly interesting because they are both cis in the native state and both occur in β-turns, but have very different effects on conformational folding. A wrong isomer of Pro114 has little effect on the folding, whereas the wrong isomer of Pro93 can slow conformational folding by 500-fold (*1*). Interestingly, Pro114 is located near a chain folding initiation site (CFIS) (*16*) which might be thought to be more sensitive to perturbations, whereas Pro93 is located in the most flexible loop of the protein [judging from its high crystallographic *B*-factors (*14*, *17*)], which might be thought to be less critical for folding. Therefore, we hoped to obtain insight into the local folding of these segments of the protein backbone by examining the effects of folding conditions on the isomerizations of their respective prolines.

MATERIALS AND METHODS

Materials. All chemicals were of the highest available quality and purity. Ultrapure grade GdnHCl was purchased from ICN Biomedicals (Aurora, OH). The plasmids for the mutants Y92F and Y115F were obtained from previous studies (*2*, *8*), and their expression and purification were carried out as described previously (*18*, *19*).

Double-Jump Unfolding Experiments. Double-jump unfolding experiments with the Y92F and Y115F mutants of RNase A (involving GdnHCl as the denaturing agent) were carried out on a Perkin-Elmer model MPF-44B dual-beam spectrofluorimeter to which a home-built double-jump mixing setup was attached. This setup consisted of two pneumatic rams (80 psi), a timer device, two mixers, a delay loop, and a flow-through quartz cuvette with a capacity of 200 μL. The temperature of the Hamilton gastight syringes and that of the flow cell were controlled independently by circulating water from refrigerated water baths. The setup was essentially similar to that described previously (*19*) except that two (instead of three) mixers were used with a delay line between them, with the first mixing producing the folding conditions (i.e., the U → F step) and the second mixing producing the final unfolding conditions (i.e., the F → U step). The final unfolded protein solution was pushed into the flow-through cell for fluorescence measurements. The excitation wavelength was 268 nm, and the fluorescence emission was collected at 302 nm, as described previously (*2*). The excitation and emission slits were adjusted so that photobleaching of the tyrosines was minimized over the longer durations required for the measurements, and a

Table 1: Denaturant Dependence of the Cis−Trans Isomerization Rates of Pro93 and Pro114 in RNase A under Folding Conditions at pH 5.0 and 15 °C

	time constant (s)	
[GdnHCl] (M)	X−Pro114	X−Pro93
0.7	73 ± 5	89 ± 19
0.9	88 ± 13	116 ± 15
1.2	148 ± 25	159 ± 19
1.5	179 ± 19	218 ± 24

Table 2: Temperature Dependence of the Cis−Trans Isomerization Rates of Pro93 and Pro114 in RNase A under Folding Conditions at 0.9 M GdnHCl and pH 5.0

	time constant (s)	
temperature (°C)	X−Pro114	X−Pro93
6	135 ± 36	−
15	88 ± 13	116 ± 15
20	−	99 ± 17
25	70 ± 6	36 ± 4

reasonably good signal-to-noise ratio was obtained. The concentration of the mutant proteins was determined by using the values of the extinction coefficients reported previously (*2*). GdnHCl concentrations were determined by measuring the refractive indices of the solutions at 25 °C using a Bausch and Lomb refractometer (*20*).

Double-jump experiments (U → F → U) have three sets of conditions: the initial unfolding conditions, the intermediate folding conditions, and the final unfolding conditions. Under the initial unfolding conditions, the protein was maintained in 4.2 M GdnHCl and 40 mM glycine-HCl buffer (pH 2.0) at a concentration of 5.4 mg/mL. In the folding (U → F) jump, 40 μL of this solution was diluted with 200 μL of the refolding buffer [80 mM sodium acetate (pH 5.3)] in a 1:5 ratio so that the pH of the mixed solution was 5.0. For some experiments, the GdnHCl concentration under the resulting intermediate folding conditions (U → F) was varied from 0.7 to 1.5 M while the temperature was held fixed at 15 °C (Table 1). In other experiments, the temperature under the intermediate folding conditions was varied from 6 to 25 °C while the GdnHCl concentration under the intermediate folding conditions was fixed at 0.9 M (Table 2). The protein was held under the intermediate folding conditions for times *t* ranging from 5 s to 20 min, after which the final unfolding (F → U) jump was carried out by diluting again in a 1:5 ratio with the unfolding buffer [4.86 M GdnHCl and 100 mM glycine (pH 1.7)] using 390 μL of flush solution (folding buffer) to push the solution for the second mixing, and 1950 μL of the unfolding buffer. The volumes of the solutions to be pushed were chosen so that the middle portion of the mixed solution was in the flow cuvette at the time of measurement. Since the unfolding buffer was identical for all experiments, the GdnHCl concentration in the final unfolding conditions varied slightly with the GdnHCl concentration in the intermediate folding conditions (from 0.7 to 1.5 M). However, this variation should not affect the results, since we have shown previously that the isomerization rates are independent of GdnHCl concentrations under unfolding conditions (*2*). The two jumps resulted in an overall 36-fold dilution of the initial protein concentration to a final concentration of 0.15 mg/mL. Changing the initial or final protein concentrations did not affect the kinetic traces significantly, and hence, the above initial and final concentrations were used in all experiments.

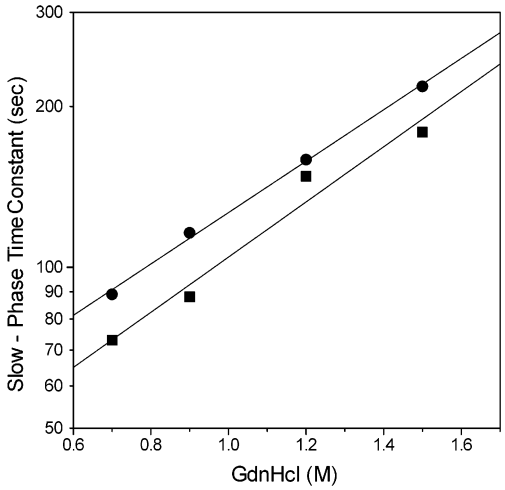

FIGURE 2: Dependence of the slow-phase time constant for X−Pro114 (■) and X−Pro93 (●) peptide bond isomerization on GdnHCl concentration at pH 5.0 and 15 °C (cf. Table 1).

Monitoring of the tyrosine fluorescence was initiated when the final unfolding jump was carried out; at least three to five shots were averaged to reduce noise. The magnitudes of the fluorescence amplitudes were obtained from the data in the kinetic traces collected over a period of 10 min in the final unfolding (F → U) step. The arbitrary values of the fluorescence amplitudes were plotted against the time *t* at which the protein was held under the intermediate folding (U → F) conditions. These plots were fitted to a single exponential using Origin™ version 2.9 graphics software from Microcal, Inc.

RESULTS

Description of the Unfolding Phases. Double-jump unfolding (i.e., interrupted folding) experiments (U → F → U) were carried out. The initially unfolded protein was subjected to folding conditions for a time *t* and then returned to unfolding conditions to assess how much of the X−Pro peptide groups had isomerized in the U → F step using our fluorescence method (*2*). In all cases, the final unfolding phases (F → U) were well-described by a single exponential with the expected time constants, roughly 115 and 45 s for the isomerization of the Tyr92−Pro93 and Asn113−Pro114 peptide bonds, respectively (*2*). The fluorescence amplitude in the final F → U step is proportional to the degree of cis−trans isomerization that occurred in the U → F step. To examine the isomerizations under folding conditions, the amplitudes of the final unfolding phases (F → U) were plotted as a function of *t*. In all the cases that were studied, the amplitudes converged to their equilibrium value at long folding times as an apparently monophasic exponential.

Effects of GdnHCl on Proline Isomerization. The isomerization rates of Pro93 and Pro114 both exhibited a dependence on the concentration of GdnHCl in the refolding buffer (Table 1 and Figure 2). In principle, this GdnHCl dependence of isomerization rates could correspond to *direct* destabilization of the isomerization transition state by GdnHCl. For example, if GdnHCl hydrogen-bonded preferentially to the carbonyl oxygen rather than the prolyl nitrogen, that would increase the double-bonded character of the peptide bond

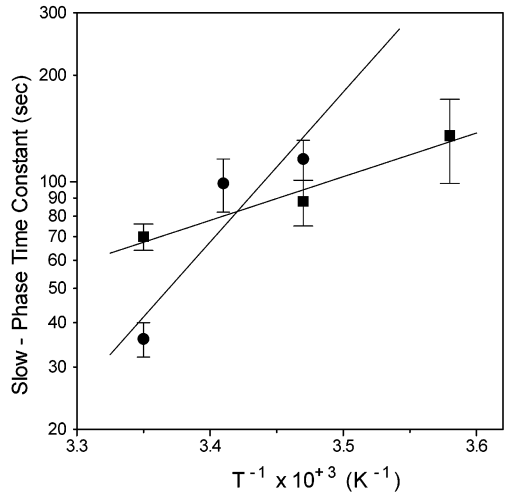

FIGURE 3: Dependence of the slow-phase time constant for X−Pro114 (■) and X−Pro93 (●) peptide bond isomerization on temperature at pH 5.0 and 0.9 M GdnHCl (cf. Table 2). These data were used to evaluate the values of the activation energy, E_a, which are 19.4 ± 8 kcal/mol for isomerization around the X−Pro93 peptide bond and 5.7 ± 1 kcal/mol for isomerization around the X−Pro114 peptide bond.

and slow the isomerization, as discussed in the introductory section. However, such a direct influence of GdnHCl is unlikely since, under unfolding conditions, both isomerizations are independent of GdnHCl concentration (*2*). Therefore, it seems that this GdnHCl dependence reflects the influence of conformational folding on the isomerizations of these two prolines.

The time constants fit well to the exponential $\tau = \tau_0 \exp(m[\text{GdnHCl}])$ for the isomerizations of the Tyr92−Pro93 and Asn113−Pro114 peptide groups under folding conditions (Figure 2). Linear regression with the semilog equation $\log \tau = \log \tau_0 + m[\text{GdnHCl}]$ yielded excellent correlation coefficients (0.999 and 0.983, respectively) with nearly identical m values (1.11 and 1.19 M^{-1}, respectively) and extrapolated zero-GdnHCl time constants (42 and 32 s, respectively). In all cases, the Pro93 isomerization was slightly slower than the Pro114 isomerization, which may reflect the influence of the preceding side chain (Tyr92 and Asn113, respectively) on the isomerization rate, as has been observed in peptide experiments (*21*, *22*).

Remarkably, the isomerization time constants measured under *weakly folding* conditions (e.g., 218 and 179 s for Pro93 and Pro114, respectively, at pH 5, 15 °C, and 1.5 M GdnHCl; see Table 1) are much higher than those measured under *unfolding* conditions (e.g., 115 and 45 s for Pro93 and Pro114, respectively, at pH 2, 15 °C, and 4.2 M GdnHCl) (*2*). By contrast, the isomerization time constants extrapolated to zero GdnHCl (i.e., under *strongly folding* conditions) are 42 and 32 s for Pro93 and Pro114, respectively, which are much lower than those observed under unfolding conditions (115 and 45 s, as above). Hence, the imposition of strongly folding conditions (specifically, low GdnHCl concentrations) accelerates the cis−trans isomerization rate of both prolines, with the isomerization of Pro93 being accelerated more strongly than that of Pro114.

Effects of Temperature on Proline Isomerization. The temperature dependence of the Pro114 isomerization under folding conditions is also unusual (Figure 3). Under folding conditions [0.9 M GdnHCl (pH 5)], Pro93 exhibits an activation energy typical of cis−trans isomerization (19.4 kcal/mol). However, analogous experiments carried out over a wide range of temperatures (6−25 °C) show that Pro114 exhibits a reduced activation energy of 5.7 kcal/mol, which is roughly the activation energy for folding of RNase A (*23*).

DISCUSSION

For brevity in the following discussion, we use the symbols U_t and U_c to denote the unfolded species having the (nonnative) trans and (native) cis isomer, respectively, of a proline; similarly, F_t and F_c denote the corresponding folded species. By definition, the native folded species F_c of Pro93 and Pro114 is more stable than the nonnative folded species F_t; hence, there are experimental conditions under which the native cis isomer is folded (i.e., F_c is more stable than U_c), but the nonnative trans isomeric species is unfolded (i.e., U_t is more stable than F_t). Such conditions are denoted here as *weakly folding* conditions. There may also be conditions under which both the native and nonnative isomeric species are folded (i.e., F_t and F_c are more stable than U_t and U_c, respectively); such conditions are denoted as *strongly folding* conditions. Finally, *unfolding conditions* are defined as those under which both isomeric species are unfolded (i.e., F_t and F_c are less stable than U_t and U_c, respectively).

It is helpful to review proline isomerization under unfolding conditions. Since the folded species are populated negligibly, the isomerization can be represented by a simple two-state kinetic model ($U_c \leftrightarrow U_t$). The net equilibration rate constant k_U is given by the sum of the forward and backward rate constants, $k_U = k_{ct} + k_{tc}$, where k_{ct} and k_{tc} represent the rate constants for the $U_c \rightarrow U_t$ and $U_t \rightarrow U_c$ steps, respectively. (The "ct" subscript signifies cis → trans isomerization, whereas the "tc" subscript signifies trans → cis isomerization.) The equilibrium constant K_U ($=[U_t]/[U_c] = k_{ct}/k_{tc}$) for this reaction is roughly 3 (*21*); i.e., the equilibrium population of U_t is roughly 3-fold that of U_c, and $k_{ct} = 3k_{tc}$. Therefore, $k_U = 4k_{tc} = (^4/_3)k_{ct}$. Since the measured equilibration time constant τ_U ($=1/k_U$) equals 115 s for Pro93 (*2*), the corresponding time constants τ_{tc} ($=1/k_{tc}$) and τ_{ct} ($=1/k_{ct}$) are roughly 460 and 153 s, respectively. Similarly, the equilibration time constant τ_U for Pro114 equals 45 s (*2*), yielding time constants τ_{tc} and τ_{ct} of roughly 180 and 60 s, respectively. These estimates of the isomerization time constants τ_{tc} and τ_{ct} will be used below.

The observed denaturant dependence of cis−trans isomerization (Table 1) is surprising for two reasons. First, such a denaturant dependence is not observed under unfolding conditions (*1*). Second, the time constants measured under strongly folding and weakly folding conditions straddle the corresponding time constants under unfolding conditions. Specifically, the isomerization time constants of Pro93 and Pro114 under weakly folding conditions (218 and 179 s, respectively, at 1.5 M GdnHCl) are *higher* than their counterparts under unfolding conditions (115 and 45 s, respectively, at 4.2 M GdnHCl). By contrast, the isomerization time constants of Pro93 and Pro114 under strongly folding conditions (42 and 32 s, respectively, extrapolated to 0 M GdnHCl) are *lower* than their counterparts under unfolding conditions (115 and 45 s, respectively, as above). This is surprising, since the isomerization time constants might be expected to change monotonically from strongly folding to weakly folding to unfolding conditions.

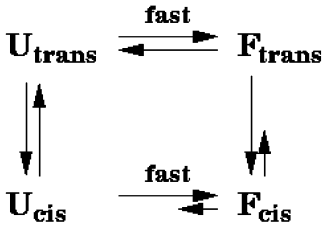

FIGURE 4: Generic reaction scheme for the coupling of conformational folding and the isomerizations of Pro93 and Pro114, which are cis in the native state.

We can explain these anomalous observations as follows. We model the isomerization under *folding* conditions according to the reaction scheme in Figure 4, where it is assumed that the folding equilibrations ($U_t \leftrightarrow F_t$ and $U_c \leftrightarrow F_c$) are much faster than the isomerization steps ($U_t \rightarrow U_c$ and $F_t \rightarrow F_c$), and the reverse reactions $F_c \rightarrow U_c$ and $F_c \rightarrow F_t$ may be neglected under folding conditions. In this kinetic model, the effective isomerization rate constant under *folding* conditions is k_F [$\approx x_F g_{tc} + x_U k_{tc}$, where g_{tc} and k_{tc} are the rate constants for the $F_t \rightarrow F_c$ and $U_t \rightarrow U_c$ reactions, respectively, and where x_F and x_U are the fractions of the (nonnative) trans isomer that are folded and unfolded, respectively, i.e., $x_F = [F_t]/([U_t] + [F_t])$ and $x_U = [U_t]/([U_t] + [F_t])$]. According to this model, the observed GdnHCl dependence of the isomerization rate constant k_F is due to the GdnHCl dependence of the fractions x_F and x_U of the folded and unfolded nonnative trans isomer.

Under strongly folding conditions, $x_F \approx 1$ and $x_U \approx 0$, which implies that $k_F \approx g_{tc}$. Hence, comparison of the isomerization time constants at zero denaturant concentrations (42 and 32 s for Pro93 and Pro114, respectively; see the third paragraph of the Results) with those under unfolding conditions (460 and 180 s for Pro93 and Pro114, respectively; see the second paragraph of the Discussion) (*2*, *8*) suggests that g_{tc} is roughly 5.6 times (180/32) greater than k_{tc} for Pro114 and roughly 11 times (460/42) greater for Pro93. In short, the imposition of folding conditions drives the isomerization of Pro93 more strongly than that of Pro114. This is consistent with NMR (*24*−*26*), X-ray (*17*, *27*), folding (*8*, *18*, *28*), and computational modeling (*29*, *30*) data showing that both isomers of Pro114 are consistent with the native fold, whereas nonnative isomers of Pro93 prevent the local backbone from forming the β-turn. For example, the Tyr92−Ala93 peptide group is cis in the P93A mutant (*17*, *26*) [although such non-prolyl cis peptide bonds are rare (*26*, *31*)], whereas the Asn113−Ala114 peptide group is trans in the P114A mutant (*18*, *27*). By contrast, under weakly folding conditions, $x_U \approx 1$ and $x_F \approx 0$, which implies that $k_F \approx k_{tc}$. The isomerization time constants under weakly folding conditions (218 and 179 s for Pro93 and Pro114, respectively, at 1.5 M GdnHCl; see Table 1) are roughly consistent with those measured under unfolding conditions (460 and 180 s for Pro93 and Pro114, respectively) (*2*, *7*).

A key question is whether the folding equilibration of the $U_t \leftrightarrow F_t$ step that affects the rates of proline isomerization represents global folding of RNase A or local ordering of the β-hairpin in which the proline is located. We argue that it is local ordering, for the following reasons. First, the equilibrium *m* values for global folding of wild-type RNase A and its mutants range from 2.4 to 4.4 (*2*), which are significantly higher than both of the isomerization *m* values measured here (1.11 and 1.19 for Pro93 and Pro114, respectively), which are relatively similar despite the different effects of these prolines on global folding (*1*). Second, no sigmoidal transition is observed in the effects of GdnHCl on the isomerization rates (Figure 2); the effects appear to be noncooperative. Third, under our folding conditions, the bulk of RNase A should have folded globally despite having nonnative proline isomers (*2*, *8*, *18*). Therefore, we conclude that our experiments are monitoring proline isomerization in RNase A molecules that are globally folded but have disordered hairpin loops due to the nonnative isomers at Pro93 and/or Pro114. In this model, the noncooperative, relatively weak GdnHCl dependence arises from the effect of the denaturant on the ordering of these hairpin loops. It is interesting to note that these hairpin loops have very different sequence compositions; the Pro114 β-hairpin is largely nonpolar, whereas the Pro93 β-hairpin is largely polar. Hence, the similarity in *m* values suggests that GdnHCl acts primarily by competing for backbone hydrogen bonds (which are common to both hairpins) rather than by modulating the solubility of their side chains (which are not).

Finally, we have yet to account for the unusual temperature dependence of the Pro114 isomerization under folding conditions. We consider it unlikely that the activation enthalpy for the isomerization of Pro114 under folding conditions is significantly different from its value (≈20 kcal/mol) under unfolding conditions (*2*). As argued above, g_{tc} is roughly 5.6 times greater than k_{tc} for Pro114, which corresponds to a free energy change of roughly 1 kcal/mol, which does not account for the 14.3 kcal/mol discrepancy between 20 kcal/mol (expected) and 5.7 kcal/mol (observed). It seems more likely that the anomalous temperature dependence results from temperature-dependent changes in the backbone dynamics that compensate for the temperature-dependent changes in the intrinsic isomerization rate constant. At higher temperatures, the proline isomerization is faster, but the unfolded state is preferred, which has a lower isomerization rate constant (e.g., greater time constants of 460 and 180 s for Pro93 and Pro114, respectively). At lower temperatures, proline isomerization is much slower but the folded state is preferred, which has a faster isomerization rate constant (e.g., 42 and 32 s for Pro93 and Pro114, respectively). These compensating changes cause the observed isomerization rate constant for Pro114 to vary less strongly with temperature than it does under unfolding conditions, leading to a reduction in the estimated activation enthalpy. This scenario may not pertain to Pro93 because the local structure is very sensitive to temperature (*32*). Elevated temperature causes disorder in the local region around Pro93, presumably making its isomerization equivalent to that which occurs under unfolding conditions, with the corresponding activation energy of 20 kcal/mol. By contrast, Pro114 is framed by a CFIS (*16*) that is by far the most stable portion of the protein under thermal denaturation (*33*).

CONCLUSIONS

We have shown that our method for monitoring cis−trans isomerizations of prolines can be extended to folding conditions. The imposition of strongly folding conditions accelerates the isomerizations of both Pro93 and Pro114, with

the isomerization rate constant g_{tc} at 0 M GdnHCl of Pro93 and Pro114 being accelerated roughly 11- and 5.6-fold, respectively, relative to the corresponding rate constant k_{tc} under unfolding conditions (4−6 M GdnHCl). Our findings are consistent with previous studies of the effects of folding conditions on the rate of proline isomerization (*34*−*36*).

However, the proline isomerization under weakly folding conditions can be even slower than under fully unfolding conditions, as has been observed for RNase T1 (*37*). The remarkably slow isomerization under weakly folding conditions may be explained by two effects. First, the net equilibration rate is the sum of the forward and backward isomerization reaction rates; even if the forward rate is faster under folding conditions, the backward rate is undoubtedly slower and may render the net sum smaller. This effect is akin to the minimum in the folding equilibration rate observed in the transition region of the well-known chevron plots. Second, the imposition of long-range constraints (such as disulfide bonds or the formation of stable native contacts) reduces the number of conformations available to the polypeptide chain and may reduce the overall rate of conformational rearrangement. However, more work will be required to characterize this second effect quantitatively, and we have not included it in our modeling.

The acceleration of isomerization by folding conditions is the counterpart of the deceleration of conformational folding by nonnative isomers of Pro93 and Pro114; a nonnative isomer of Pro93 retards conformational folding 500-fold, while a nonnative isomer of Pro114 retards conformational folding roughly 2-fold at pH 5.0 (*2*, *8*, *28*). More generally, we conclude that folding conditions can promote *specific* local backbone structure in segments of the backbone, and that specific structure in these segments can be critical for conformational folding. These conclusions are consistent with studies of protein L in which the folding rate was increased 100-fold by redesigning a single β-hairpin to dispose that hairpin to fold locally (*38*) and with other experiments that show large increases in folding rates when the native secondary structure is stabilized (*39*), as well as many studies of peptides showing strong local structural propensities in naturally occurring proteins (*40*). However, not all local structure is equally important for folding; for example, disordered segments persist in many folded proteins (*41*), and folding is unaffected by nonnative isomers of many prolines (*1*). Pro114 is a good example, because it is adjacent to the most important CFIS (the C-terminal β-hairpin) of RNase A (*16*) and yet the nonnative isomer of Pro114 affects folding little, because the key hydrophobic contacts and hydrogen bonds of the CFIS can form with both the native and nonnative isomer (*8*, *18*, *24*−*30*). These conclusions are consistent with traditional (multi)nucleation-type models (*16*, *42*−*44*) but contradict recent "smooth funnel" models proposing that the folding transition state has no specific backbone structure, only a roughly correct topology that is determined primarily by side chain−side chain interactions (*45*).

ACKNOWLEDGMENT

We thank Ervin Welker and Mahesh Narayan for critical reading of the manuscript and helpful discussions during the course of this study and V. Gary Davenport for technical assistance.

REFERENCES

1. Wedemeyer, W. J., Welker, E., and Scheraga, H. A. (2002) *Biochemistry 41*, 14637−14644.
2. Juminaga, D., Wedemeyer, W. J., and Scheraga, H. A. (1998) *Biochemistry 37*, 11614−11620.
3. Iwaoka, M., Wedemeyer, W. J., and Scheraga, H. A. (1999) *Biochemistry 38*, 2805−2815.
4. Drakenberg, T., Dahlqvist, K.-I., and Forsén, S. (1972) *J. Phys. Chem. 76*, 2178−2183.
5. Steinberg, I. Z., Harrington, W. F., Berger, A., Sela, M., and Katchalski, E. (1960) *J. Am. Chem. Soc. 82*, 5263−5279.
6. Texter, F. L., Spencer, D. B., Rosenstein, R., and Matthews, C. R. (1992) *Biochemistry 31*, 5687−5691.
7. Eberhardt, E. S., Panasik, N., Jr., and Raines, R. T. (1996) *J. Am. Chem. Soc. 118*, 12261−12266.
8. Juminaga, D., Wedemeyer, W. J., Garduño-Júarez, R., McDonald, M. A., and Scheraga, H. A. (1997) *Biochemistry 36*, 10131−10145.
9. Itzhaki, L. S., Otzen, D. E., and Fersht, A. R. (1995) *J. Mol. Biol. 254*, 260−288.
10. Riddle, D. S., Grantcharova, V. P., Santiago, J. V., Alm, E., Ruczinski, I., and Baker, D. (1999) *Nat. Struct. Biol. 6*, 1016−1024.
11. Kim, D. E., Fisher, C., and Baker, D. (2000) *J. Mol. Biol. 298*, 971−984.
12. Neira, J. L., and Rico, M. (1997) *Folding Des. 2*, R1−R11.
13. Raines, R. T. (1998) *Chem. Rev. 98*, 1045−1065.
14. Wlodawer, A., Svensson, L. A., Sjölin, L., and Gilliland, G. L. (1988) *Biochemistry 27*, 2705−2717.
15. Koradi, R., Billeter, M., and Wüthrich, K. (1996) *J. Mol. Graphics 14*, 51−55.
16. Matheson, R. R., Jr., and Scheraga, H. A. (1978) *Macromolecules 11*, 819−829.
17. Pearson, M. A., Karplus, P. A., Dodge, R. W., Laity, J. H., and Scheraga, H. A. (1998) *Protein Sci. 7*, 1255−1258.
18. Dodge, R. W., and Scheraga, H. A. (1996) *Biochemistry 35*, 1548−1559.
19. Houry, W. A., and Scheraga, H. A. (1996) *Biochemistry 35*, 11734−11746.
20. Nozaki, Y. (1972) *Methods Enzymol. 26*, 43−50.
21. Grathwohl, C., and Wüthrich, K. (1981) *Biopolymers 20*, 2623−2633.
22. Reimer, U., Scherer, G., Drewello, M., Kruber, S., Schutkowski, M., and Fischer, G. (1998) *J. Mol. Biol. 279*, 449−460.
23. Houry, W. A., Rothwarf, D. M., and Scheraga, H. A. (1994) *Biochemistry 33*, 2516−2530.
24. Stimson, E. R., Montelione, G. T., Meinwald, Y. C., Rudolph, R. K. E., and Scheraga, H. A. (1982) *Biochemistry 21*, 5252−5262.
25. Montelione, G. T., Arnold, E., Meinwald, Y. C., Stimson, E. R., Denton, J. B., Huang, S.-G., Clardy, J., and Scheraga, H. A. (1984) *J. Am. Chem. Soc. 106*, 7946−7958.
26. Xiong, Y., Juminaga, D., Swapna, G. V. T., Wedemeyer, W. J., Scheraga, H. A., and Montelione, G. T. (2000) *Protein Sci. 9*, 421−426.
27. Schultz, D. A., Friedman, A., and Fox, R. O. (1993) *Protein Sci. 2* (Suppl. 1), 67.
28. Houry, W. A., and Scheraga, H. A. (1996) *Biochemistry 35*, 11719−11733.
29. Pincus, M. R., Gerewitz, F., Wako, H., and Scheraga, H. A. (1983) *J. Protein Chem. 2*, 131−146.
30. Oka, M., Montelione, G. T., and Scheraga, H. A. (1984) *J. Am. Chem. Soc. 106*, 7959−7969.
31. MacArthur, M. W., and Thornton, J. M. (1991) *J. Mol. Biol. 218*, 397−412.
32. Schmid, F. X. (1981) *Eur. J. Biochem. 114*, 105−109.
33. Burgess, A. W., and Scheraga, H. A. (1975) *J. Theor. Biol. 53*, 403−420.
34. Cook, K. H., Schmid, F. X., and Baldwin, R. L. (1979) *Proc. Natl. Acad. Sci. U.S.A. 76*, 6157−6161.
35. Schmid, F. X. (1986) *FEBS Lett. 198*, 217−220.
36. Sendak, R. A., Rothwarf, D. M., Wedemeyer, W. J., Houry, W. A., and Scheraga, H. A. (1996) *Biochemistry 35*, 12978−12992.

37. Mücke, M., and Schmid, F. X. (1994) *J. Mol. Biol. 239*, 713−725.
38. Nauli, S., Kuhlman, B., and Baker, D. (2001) *Nat. Struct. Biol. 8*, 602−605.
39. Chiti, F., Taddei, N., Webster, P., Hamada, D., Fiaschi, T., Ramponi, G., and Dobson, C. M. (1999) *Nat. Struct. Biol. 6*, 380−387.
40. Montelione, G. T., and Scheraga, H. A. (1989) *Acc. Chem. Res. 22*, 70−76.
41. Dunker, K., and Obradovic, Z. (2002) *Hum. Genome News 12*, 13−14.
42. Lewis, P. N., Momany, F. A., and Scheraga, H. A. (1971) *Proc. Natl. Acad. Sci. U.S.A. 68*, 2293−2297.
43. Ptitsyn, O. B. (1973) *Dokl. Akad. Nauk SSSR 210*, 1213−1215.
44. Anfinsen, C. A. (1973) *Science 181*, 223−230.
45. Dill, K. A. (1999) *Protein Sci. 8*, 1166−1180.

BI030024T